Fine metal dust particles on the wall probes from JET-ILW

Fine metal dust particles on the wall probes from JET-ILW

E. Fortuna-Zaleśna[a*], J. Grzonka[a,b], M. Rubel[c], Sunwoo Moon[c], P. Petersson[c], A. Widdowson[d] and JET Contributors**

EUROfusion Consortium, JET, Culham Science Centre, OX14 3DB, Abingdon, UK
[a]Faculty of Materials Science and Engineering, Warsaw University of Technology, Warsaw, Poland
[b]Institute of Electronic Materials Technology, Warsaw, Poland
[c]Royal Institute of Technology (KTH), SE-10044 Stockholm, Sweden
[d]Culham Centre for Fusion Energy, Culham Science Centre, Abingdon, OX14 3DB, UK

***See the author list in: X. Litaudon et al., Nuclear Fusion Special issue: 26th Fusion Energy Conference (Kyoto, Japan, October 2016)*

Abstract

Collection and ex-situ studies of dust generated in controlled fusion devices during plasma operation are regularly carried out after experimental campaigns. Herewith results of the dust survey performed in JET after the second phase of operation with the metal ITER-Like Wall (2013-2014) are presented. Particles deposited on silicon plates acting as dust collectors installed in the inner and outer divertor have been examined. The emphasis is on analyzing metal particles (Be and W) with the aim to determine their composition, size and surface topography. The most important is the identification of beryllium dust in the form of droplets (both splashes and spherical particles), flakes of co-deposits and small fragments of Be tiles. Tungsten and nickel rich (from Inconel) particles are also identified. Nitrogen from plasma edge cooling has been detected in all types of particles. They are categorized and the origin of various constituents is discussed.

Keywords: *plasma, dust, JET tokamak, ITER-Like Wall, beryllium, tungsten*

PACS: 52.40.Hf

*Corresponding author: tel.: +48 22 234 87 48, e-mail: efortuna@o2.pl (E.Fortuna-Zalesna)

1. Introduction

Dust generation accompanying plasma operation is observed in low- and high-temperature systems, i.e. both in laboratory or industrial plasma chambers and in reactors of controlled thermonuclear fusion (CTF). This work is focused on phenomena occurring in CTF devices with magnetic plasma confinement. Concerns regarding reactor safety and diagnostic performance in a reactor-class device are the main driving forces for dust studies in current machines. Dust surveys have been carried out regularly at several tokamaks: TEXTOR [1-3], ASDEX-Upgrade [4-6], JET [7-9] and other machines. Most works performed in this field until the end of year 2011 have been referenced by Braams [10]. Detailed knowledge of dust generation is important for licensing and future operation of ITER (International Thermonuclear Experimental Reactor). JET tokamak at the Culham Science Centre, United Kingdom) is the most relevant machine from the ITER point of view because of the full metal wall composed of beryllium in the main chamber wall and tungsten in the divertor, the ITER-Like Wall (JET-ILW) operated since 2011 [11]. Collection of dust after the first campaign (ILW-1, 2011-2012) has shown small overall quantity of loosely bound species in the divertor (below 1 g) [7]. In addition, a limited local (only from apron Tile 1) [8,9] sampling by adhesive tape allowed for the identification of several classes of particles which were ITER-relevant, e.g. flakes of Be-rich deposits, and also those which are not expected to be present in a reactor-class machine: pieces of tungsten coatings, small debris of carbon fibres from the W-coated tiles or boron nitride from the fast reciprocating probe heads.

After the second ILW campaign (ILW-2, 2013-2014) global collection by vacuum cleaning of the divertor surface (below 1.5 g) [9,12] was complemented by a comprehensive sampling of dust and co-deposits from tiles using adhesive carbon pads [9]. The third approach is the search for particles on dust monitors (collectors) and on surfaces of other erosion-deposition probes (EDP) [13], e.g. test mirrors [14]. This contribution is focused on the analyses of dust collected on the wall probes. Such particles give unique insight into the properties (size, composition, structure) of the mobilized dust, especially metal droplets. It also gives a hint on statistics. These are the first data from JET on single objects migrating in the vacuum vessel and not disintegrated or modified by the collection; i.e. particles are in the form and place as they were deposited. Comprehensive characterization of metal particles, especially beryllium, is the main aim of the work.

2. Experimental

The study was carried for particles deposited on two silicon dust monitors/collectors retrieved from JET after the second ILW campaign in 2013-2014 which comprised 19.5 h of plasma operation (13.5 h of X-point plasma) with total energy input of 201 GJ. Monitors were placed on the high- and low-field sides of the vessel, respectively, above the inner and outer divertor plates but below the arrays of poloidal limiters. These were steel boxes with silicon plates acting as dust collecting surfaces. They were designed and manufactured at the Max Planck Institute of Plasma Physics (Garching, Germany) and tested earlier during experimental campaigns in ASDEX Upgrade [5]. For the use at JET the construction was modified to be compatible with remote handling. The wall structure and details regarding the collectors and their installation shown in images presented in Fig.1. The collector on the inner wall (Octant 6) was placed below the inner wall cladding, while on the outer wall (Octant 2) it was in the saddle coils below the antenna for ion cyclotron resonance frequency (ICRF) heating. The study of silicon plates has been complemented by the examination of species deposited on wall probes, e.g. surfaces of test mirrors [14,15].

The morphology (structure, size, composition) of single dust particles and splashes on various wall probes was examined at the Warsaw University of Technology (Poland) using scanning electron microscopy (SEM, Hitachi SU-8000 FE-SEM) combined with energy-dispersive X-ray spectroscopy enabling beryllium detection (EDS, Thermo Scientific Ultra Dry, type SDD – silicon drift detector) and focused ion beam (FIB, Dual Beam Hitachi NB5000). The composition and depth profiles of species in co-deposits formed on the probes were determined with ion beam analysis (IBA) techniques (Ångström Laboratory, Uppsala University, Sweden) such as nuclear reaction analysis (NRA) with a $^{3}He^{+}$ beam and time-of-flight heavy ion elastic recoil detection analysis (ToF HIERDA) with a 36 MeV iodine ($^{127}I^{8+}$) beam. The analyses were performed in a few areas on each of the studied specimens using high-resolution detector described in [16].

3. Results and discussion

3.1. Deposition on dust monitors: general features

Visual inspection of the monitors indicated the presence of thin deposited layers and only very few isolated particles which could be considered as dust. Results of the quantitative depth profiling with ToF HIERDA are in Fig. 2. Features of all co-deposited species are recorded: from hydrogen to Inconel wall components (Ni and Fe) and traces of tungsten. The hydrogen signal is significantly stronger than that of deuterium reflecting the fact that the

ILW-2 campaign was concluded with approximately 300 shots in hydrogen fuel which resulted in the depletion of the D content in deposits on limiters by 30% in comparison to the retention after ILW-1 [12,17,18]. The presence of nitrogen puffed for plasma edge cooling is clearly noticed. The strongest signal is related to silicon from the substrate, thus proving that the layer thickness does not exceed 1 μm, i.e. which is the reliable information depth with HIERDA in layers composed mainly of low-Z atoms. Depth profiles in Fig. 2 (b) for the outer divertor confirm small thickness of co-deposits. Beryllium is the major species (40%), but the contribution of Inconel constituents is remarkably high. Their origin on the outer wall monitor is most probably connected to: (a) the erosion at the Inconel ICRF grill and (b) the unfortunate damage and melting of tie rods in the vertical divertor tiles (Tile 7) and consecutive spreading of Ni and Fe onto the horizontal Tile 6. Erosion of the vacuum vessel wall also contributes to the generation of medium-Z impurities. For clarity of presentation the profiles of carbon and oxygen are not depicted: the concentration of these elements in the co-deposited layer amounts to about 10 and 30%, respectively.

Overview microscopy images have revealed that collectors are covered with a large number of small particles: approximately 300 – 500 per mm^2. Their analysis is reported in the following chapters.

3.2. Beryllium

Five types of beryllium-rich particles have been identified: (i) Be splashes and (ii) small spheres both related to melting events on the limiters, (iii) flakes of co-deposits; (iv) small quantity of little fragments of beryllium tiles and (v) coatings detached from the inner wall cladding tiles. Only three first three categories are ITER-relevant. The occurrence of the fourth class is probably unavoidable in connection with the tile installation or removal but it is neither related to discharges nor crucial to the plasma operation as long as the amounts of such matter are small. The fifth category, shown already in [9], will not be discussed here because it is specific only to JET where 8 μm thick coatings were deposited to mask Inconel inner wall cladding tiles [19]. It is worth stating that the occurrence of flakes detached from the coatings is very rare in the studied monitors thus indicating durability of the evaporated Be films.

Some tens (over 50) of beryllium splashes and spherical droplets have been studied in detail. Many more have been briefly inspected. It is stressed that the analysis of beryllium-containing particles cannot be automated, because the energy of emitted X-rays is very low,

$K_{\alpha(Be)}$ =108 eV, and this has an impact on the detection sensitivity. As a result, each particle required individual attention of the microscope operator to ensure proper identification and classification of the objects: droplet, thin splash, co-deposited Be. The additional difficulty in the interpretation of EDS data has been related to a very small size or small thickness of most objects. On many instances the X-rays generated from the underlying silicon constituted the major feature in the energy spectrum.

3.2.1 Inner wall dust monitor

Particles distributed uniformly on the entire surface of the monitor from the inner wall are mainly beryllium splashes. Images in Fig. 3 show a number of objects recorded at different view angles. Splashes are fairly circular ("pancake-like" shape) with a diameter between 10 μm and 130 μm. The most typical size range is between 25 μm and 40 μm (over 50% of the examined particles). From images recorded at the oblique angle one infers that a molten metal was still flowing after hitting the collector plate. As a result there are "tentacles" and – in all cases – the presence of an elevated rim surrounding the central part of splashes. There are numerous cracks developed during metal cooling on a cold (around 150 ^{o}C) collector but despite internal stresses the splashes adhere well to the substrate. Cross-sections produced by FIB, an example is shown in Fig. 4, for several particles bring a set of crucial information on: (i) the internal structure; (ii) surface layer free from a film of co-deposited species; (iii) the thickness.

The fairly uniform internal structure without a split into thin strata clearly confirms that the "pancakes" were formed in a single event, not as a result of gradual deposition over a longer period. The lack of noticeable co-deposited layers provides a strong indication that splashing occurred at the final stages of the ILW-2 campaign. With very high probability it may be attributed to the experiment performed on the last operation day: generation of run-away electrons. High power loads at disruptions caused melting of the upper dump plates (UDP). As a consequence, there was a "rain" of droplets falling at right angle (straight down) from the molten layer of dump plates located just above the monitor on the high field side. Images showing the damage at UDP are in Fig. 5. This explains a circular shape of splashes on that collector. The shape makes these particles distinct in comparison to elongated, even comet-like, metal splashes recorded on earlier occasions when the $\boldsymbol{j \times B}$ force played strong role [1,2]. Though the effect of UDP melting is clearly seen it is not possible to conclude whether (and *if*, then to which extent) the matter from the plates was lost or only displaced. High-resolution photographic survey of the entire vessel also enabled identification of

droplets released from the UPD and deposited on the high field gap closure tile (HFGC, Tile 0) in the inner divertor and on surfaces in the vicinity on the dust collector.

The dimensions (radii [r], thickness [d]) of splashes allow for the estimation of the size range and mass of droplets reaching the collector. The density of beryllium is taken as 1.8 g cm^{-3}, i.e. between density for the liquid at the melting point (1.69 g cm^{-3}) and the solid (1.848 g cm^{-3}) [20]. Examples for several sizes are collected in Table 1.

Table 1

Splash radius (μm)	Splash thickness (μm)	Droplet volume (10^{-9} cm^3)	Mass (ng)	Droplet radius (μm)
5	0.4	0.03	0.056	1.9
20	0.6	0.75	1.36	5.6
65	0.8	106.3	191	29,4

Taking into account the average size of splashes (r = 20 μm, d = 0.6 μm), the population of such particles (300 mm^{-2}) and the surface area of the inner divertor (12.5 m^2) one may estimate the amount of beryllium removed from the UDP and converted into droplets by the disruption: 0.52 g corresponding to the volume (V) of about 0.3 cm^{-3}.

Identification of spherical Be droplets (3-8 μm in diameter) has already been documented after ILW-1 [8,9]. Such objects, all of them fairly small (1.5-4 μm in diameter), of nearly perfect spherical shape have been found also on the monitors. Two particles are shown in Fig. 6(a) and (b). Their masses and volumes are in the range from $3.3x10^{-3}$ ng (V = $1.8x10^{-12}$ cm^3) to $5x10^{-2}$ ng (V=$28x10^{-12}$ cm^3). No bigger spherical Be droplets have been detected. All numbers given above are judged to be small, but it should be taken into account that the formation of the studied splashes and droplets has been most probably related to only a single event. On spheres' surfaces one perceives small pits. It is difficult to give a decisive answer about the cause of such structures, but they may be related to the release of gases (hydrogen isotopes and/or nitrogen) from hot droplets. This statement is supported by the detection of bubbles related most probably to beryllium still boiling in splashes on the test mirror from the main chamber and in deposits detached from the divertor tiles. The latter is documented in Fig. 6(c).

3.2.2. Outer wall dust monitor

The areal density of particles on the monitor at the outer wall is similar to that on the inner, 300-500 particles per mm^2, but certain qualitative differences are noticed when a

comparison is done. The number of Be splashes (some of them elongated) is significantly smaller than on the inner, but instead the population of spherical droplets (up to 10 μm in diameter) is larger. Most of them are at least partly coated by tiny flakes of co-deposits, as shown in Fig. 7(a) together with X-ray spectrum, indicating that their formation could occur earlier than on the last operation day in ILW-2. They might be formed in melting events of outer poloidal limiters. In addition to the Be droplets, there are single flakes (size range: 5 - 100 μm) of co-deposits detached most probably from the deposition zones on limiters, as illustrated in Fig. 7(b).

Agglomerates constitute a separate group of objects. Images in Fig. 8 (a) and (b) show a particle composed of a tight beryllium mantle and a porous interior with carbon and Inconel, as proven by EDS on a FIB-produced cross-section. A number of such agglomerates, some with featureless glass-like surfaces, have been found. Their interior may vary, e.g. fine silicon or silicon-magnesium from ceramics. A common feature is a tight and uniform Be mantle whose presence suggests that the trapped species were mobile (moving on the dust monitor surface) during the Be deposition until they got immobilized; the fibrous links binding a particle to the surface are indicated with an arrow.

3.2. Inconel and tungsten

Plentiful spherical nickel (Inconel) droplets and ball-like structures originating from tungsten coatings complement the spectrum of objects presented in this paper. Other metal pieces, such as swarf, will not be discussed as their origin is not related to plasma operation.

Images of Inconel (Ni and Fe found by EDS) particles collected in Fig. 9(a)-(d) show respectively: a 300 nm wide comet-like droplet, a 100 μm long splash and spherical droplets. Two examples are demonstrated: nearly bare sphere on the outer wall dust monitor with only some traces of low-Z deposits (Fig. 9c) and a droplet tightly covered by beryllium deposit on the apron of Tile 1 in the inner divertor (Fig. 9d). The latter one is just proving that it was residing on the tile for quite time. It means that various Inconel droplets detected in JET were formed during different events. In general, majority of nickel-containing particles on the monitors and in other locations are very small (below 10 μm), while objects like the one in Fig. 9(b) are rather exceptional.

Tungsten spheroids, i.e. ball-like objects with a thin shell and empty interior, have been detected after ILW-2 in significant quantities (observation after ILW-1 in [8]). They originate from tungsten flakes detached by whichever reason from the W coatings on carbon

fibre composite (W/CFC) tiles in the divertor or in the beam shine-through protection region of the JET wall. Some options regarding the nucleation and growth processes of such objects were proposed and discussed in [8]. After ILW-2 they have been found on the divertor tiles, on dust monitors and also on test mirrors located deep in the shadowed region of the divertor. A collection of pictures selected from a large catalogue is in Fig. 10. Images show closed spheres and also demonstrate objects *in statu nascendi*. In that phase, thin W flakes start forming round structures acting as "scaffolding" for next pieces in the scrape-off layer (SOL) to merge the precursor and coagulate. One may suggest that the process leads to the decrease of area in contact with plasma. A good insight into the internal structure is provided in Fig. 10(d) where a cross-section of the shell is visible. The outer diameter of the ball is around 2.2 μm, the shell thickness is 0.3-0.4 μm and the resulting volume of W in the shell is 3.8×10^{-12} cm^3. Assuming porosity in the structure at about 20%, the mass of the "ball" would be around 56×10^{-12} g corresponding roughly to less than 2×10^{11} W atoms. Such objects, as derivatives of coatings, are not ITER-relevant. However, they are presented here for a single reason: without proper SEM/FIB studies they might mistakably be considered as W droplets and serve for reactor-directed predictions or modelling.

4. Concluding remarks

For the first time a broad survey of as-deposited (i.e. not affected or modified by the collection method) on the wall components dust particles from JET with the ITER-Like Wall has been possible due to the analyses of dust monitors. The main aim of work, i.e. detailed determination of metal particles, has been achieved. The location of monitors above the divertor has allowed for the collection of species formed under plasma operation especially in the main chamber and then mobilized by plasma. The production of beryllium droplets, deposited in the form of spherical or flat splashed objects, has been clearly demonstrated. The structure and surface state (free from other deposits) of those particles suggests that their generation took place as a result experiments aiming at run-way electrons production on the last day of ILW-2 campaign. An attempt to estimate the amount of matter released and then deposited by such melt events brings numbers (around 0.52 g corresponding to 0.3 cm^{-3} of Be) which are judged to be small. However, it should be taken into account that the formation of the studied splashes and droplets has been most probably related to only a single event. For various reasons (e.g. wall structure) the extrapolation to ITER is neither intended nor attempted here, but that observation from JET signifies the fact that local material losses at high power off-normal events, which may and certainly will take place in a reactor, will have

direct impact on the target thickness and, as consequence, thermo-mechanical performance of the components.

The study has revealed the presence of several other classes of particles on the monitors, such as nickel (Inconel) regular spherical droplets, agglomerates of various species (W, Ni, ceramics) tightly coated by beryllium deposits and, as expected, flakes of co-deposited layers peeled-off from plasma-facing components. New and better insight has been obtained to the formation of tungsten ball-like objects originating from thin flakes of W coatings in JET. These objects are not important from the reactor point of view, as no coatings are planned. Examination of such species has derived from a very careful search for solid W droplets and/or splashes. There is lack of any evidence of bulk tungsten objects. This statement is based on all results of dust studies from the JET-ILW, i.e. current study and those presented in [8,9,21]. One may assume that both from the JET and ITER perspective it is a very positive result. It shows that the formation of W droplets in JET took only place on tungsten components protruding from the divertor structure: Langmuir probes and special lamellae in Tile 5 (bulk W tile in the JET divertor) used in dedicated melt experiments [22].

Acknowledgement

This work has been carried out within the framework of the EUROfusion Consortium and has received funding from the European Union's Horizon 2020 research and innovation programme under grant agreement number 633053. The views and opinions expressed herein do not necessarily reflect those of the European Commission.

References

1. Ivanova D *et al* 2009 Phys. Scr. **T138** 014025
2. Fortuna-Zalesna E *et al* 2016 Phys. Scr. **T167** 014059
3. Fortuna E *et al* 2007 *J. Nucl. Mater*. **367–370** 1507
4. Fortuna-Zalesna E *et al* 2014 *Phys. Scr*. **T159** 014066
5. Balden M *et al* 2014 *Nucl. Fusion* **54** 073010
6. Endstrasser N *et al* 2011 *J. Nucl. Mater.* **415** S1085
7. Widdowson A et Phys. Scr. (2014) T159 014010.
8. Baron–Wiechec A *et al* 2015 *Nucl. Fusion* **55** 113033.
9. Fortuna E *et al* 2017 *Nucl. Mat. Energy* http://doi.org/10.1016/j.nme.2016.11.027

10. Braams B *Characterisation of Size, Composition and Origins of Dust in Fusion Devices*, IAEA, 2012, *http://www-nds.iaea.org/reports-new/indc-reports*
11. Matthews G F *et al* 2011 *Phys. Scr.* **T145** 014001.
12. Widdowson A *et al* 2017 *Nucl. Fusion* in press
13. Rubel M *et al* 2013 *J. Nucl. Mater.* **438** S1204
14. Garcia-Carrasco A *et al* 2017 *Nucl. Mater. Energy* http://doi.org/10.1016/j.nme.2016.12.032
15. Ivanova D *et al* (2014) *Phys. Scr.* **T159** 014011
16. Ström P *et al* 2016 *Rev. Sci Instrum.* **87** 103303
17. Rubel M *et al* 2017 *Nucl. Fusion* **57** 066027
18. Litaudon X *et al* 2017 *Nucl. Fusion* in press
19. Rubel M *et al* 2008 *J. Phys. Conf. Series* **100** 062028
20. Greenwood NN, Earnshaw A 1988 *Chemie der Elemente*, 1st Edition, VCH, Weinheim, ISBN 3-527-26169-9, p. 136.
21. Ashikawa N *et al* 2016 *Comprehensive analysis of dust particles from JET-ILW and impact of fusion reactor*, Proc. 26th IAEA Fusion Energy Conf. , EX/P6-1, Kyoto, Japan
22. Coenen JW *et al* 2017 *Transient induced tungsten melting at the Joint European Torus (JET)*, 16th Int. Conf. Plasma-Facing Materials and Components, Neuss, Germany

Figure captions

Fig. 1. Map of components inside the JET vacuum vessel: (a) four octants of the low-field-side and (b) all eight octants of the high-field side. The position of dust monitors is marked with red circles. Wall components: (1) Inner Wall Guard Limiters, (2) saddle coils and their protection limiters, (3) lower hybrid antenna, (4) ICRF antenna (5) outer divertor tiles. Details of dust monitors: (c) a scheme of the box, (d) a scheme of the installation, (e) collector plate and (f) monitor installed above the inner divertor.

Fig. 2. Results of the silicon plate analysis with ToF HIERDA: (a) spectrum with described detected elements and (b) depth profiles for Be, Ni, N and Si.

Fig. 3. Micrographs of beryllium splashes on the inner wall monitor. Images were taken at (a) and (b) normal angle and (c) and (d) at 58^{o}.

Fig. 4. Cross-section obtained by focused ion beam of a beryllium splash on the inner wall monitor. Thickness of the layer in various places is marked.

Fig. 5. Top part of the JET vacuum vessel with beryllium upper dump plates: (a) an overview image and (b) details of the molten region.

Fig. 6. (a) and (b) Spherical beryllium droplets on the dust monitor; (c) beryllium bubbles in the Be-rich deposit on the divertor tile.

Fig. 7. (a) Beryllium droplet coated with a co-deposit (b) beryllium- rich flake. Both from the outer wall monitor. Corresponding X-ray spectra are also presented.

Fig. 8. Agglomerated dust particles on the outer wall monitor: (a) whole particle and (b) a cross-section obtained by FIB.

Fig. 9. Splashes and regular spherical droplets of medium-Z metals: (a) and (b) nickel (Inconel) splashes of various size on the on inner wall dust monitor; (c) iron droplet on the outer wall monitor; (d) nickel(Inconel droplet) coated with Be-rich deposit on the apron of Tile 1 in the inner divertor.

Fig. 10. Tungsten ball-like structures with a thin shell and empty interior: (a) and (b) closed spheres, (c) sphere in the phase of formation and (d) broken shell. Particles (a) – (c) are from the outer wall monitor while (d) is from the test mirror in the divertor.

Figure 1

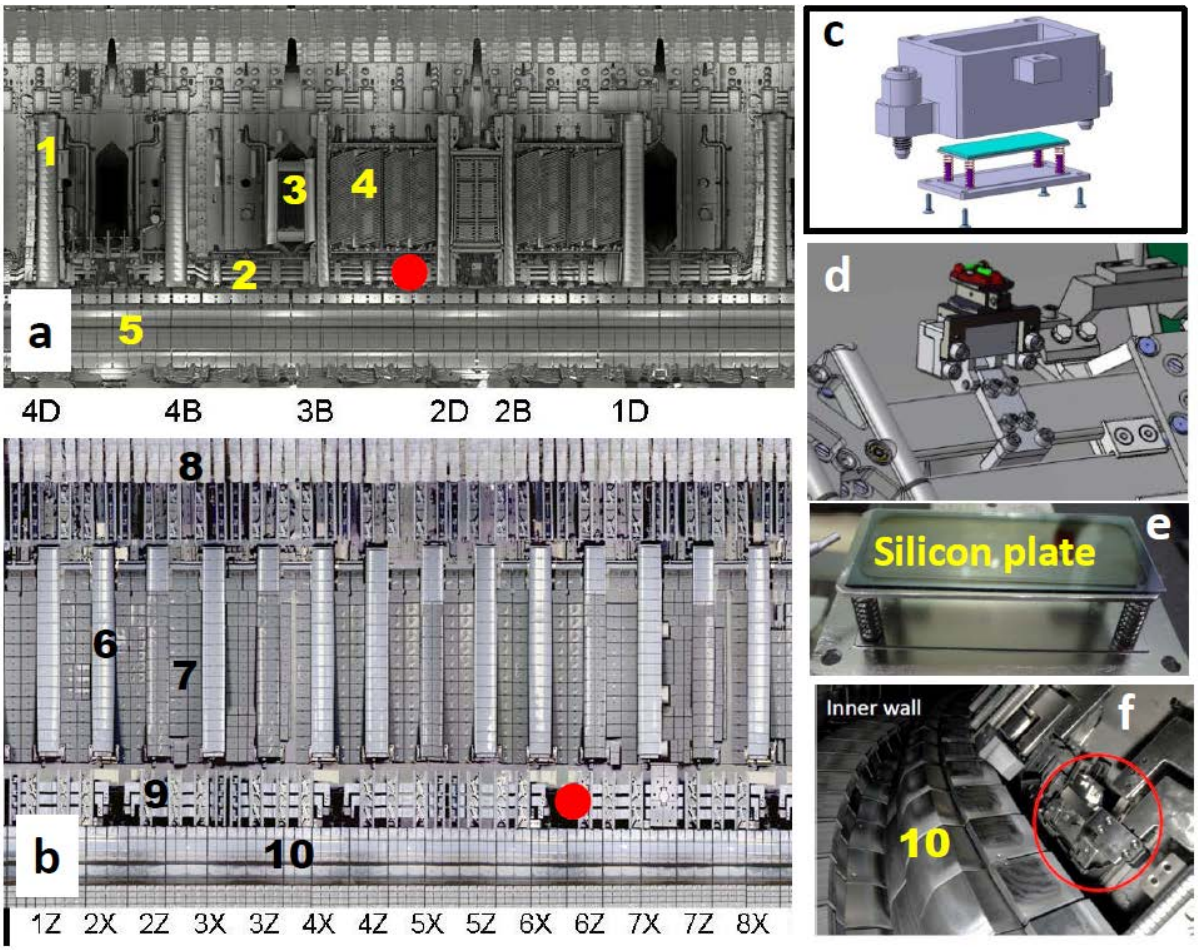
a
1
2
3
4
5
4D
4B
3B
2D
2B
1D
b
6
7
8
9
10
1Z
2X
2Z
3X
3Z
4X
4Z
5X
5Z
6X
6Z
7X
7Z
8X
c
d
e
Silicon plate
f
Inner wall
10

Figure 2

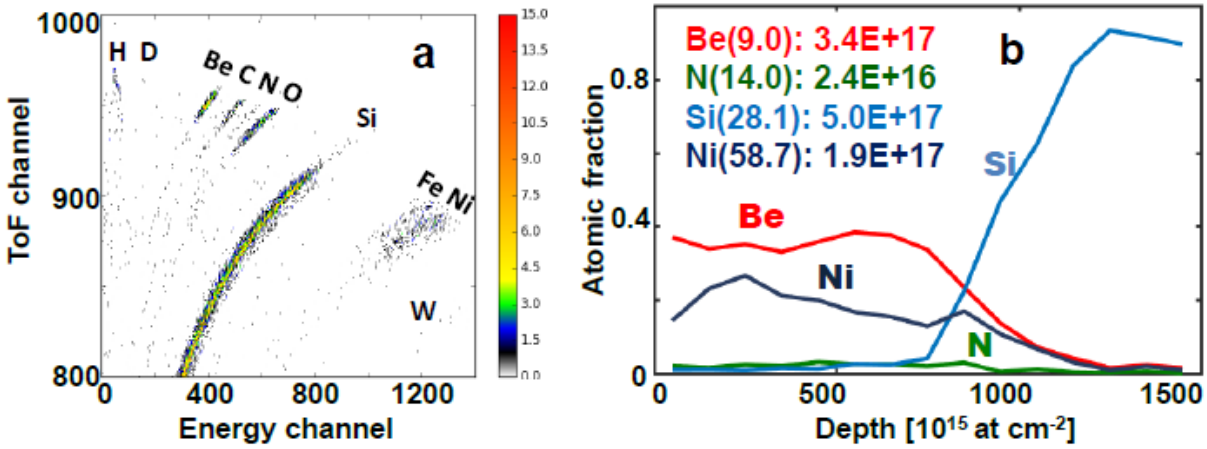
a
H D
Be C N O
Si
Fe Ni
W
ToF channel
Energy channel
1000
900
800
0
400
800
1200
15.0
13.5
12.0
10.5
9.0
7.5
6.0
4.5
3.0
1.5
0.0
b
Be(9.0): 3.4E+17
N(14.0): 2.4E+16
Si(28.1): 5.0E+17
Ni(58.7): 1.9E+17
Si
Be
Ni
N
Atomic fraction
0.8
0.4
0
500
1000
1500
Depth [10^15 at cm^-2]

Figure 3

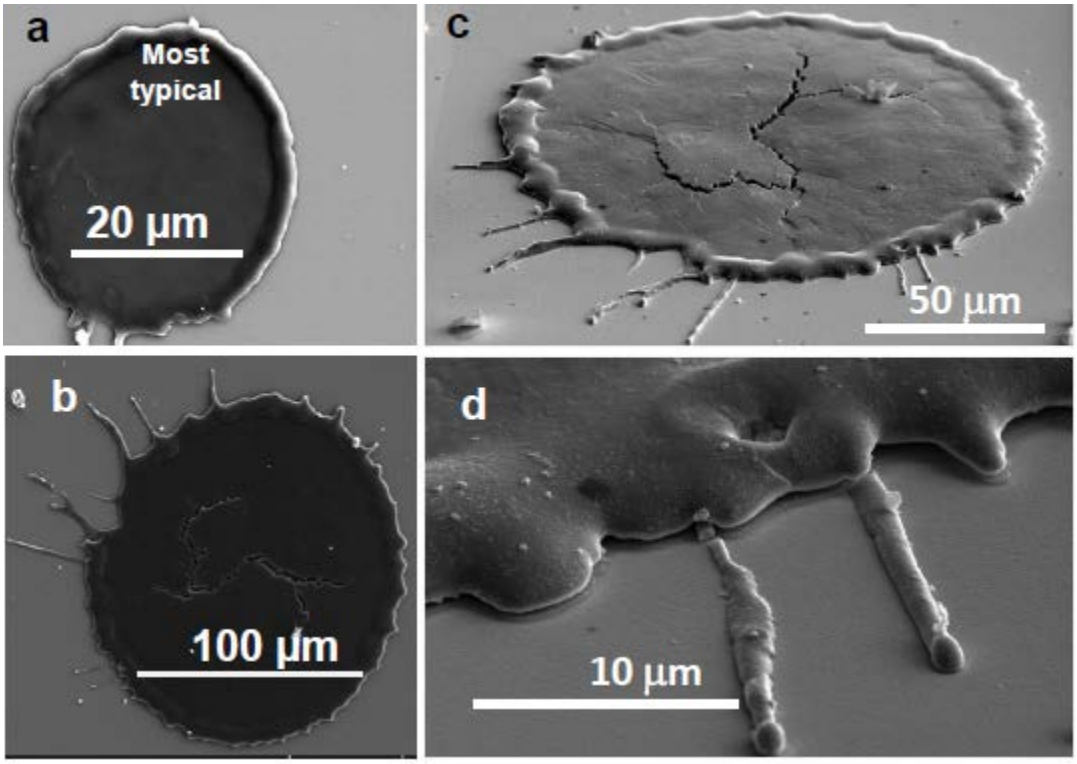

Figure 4

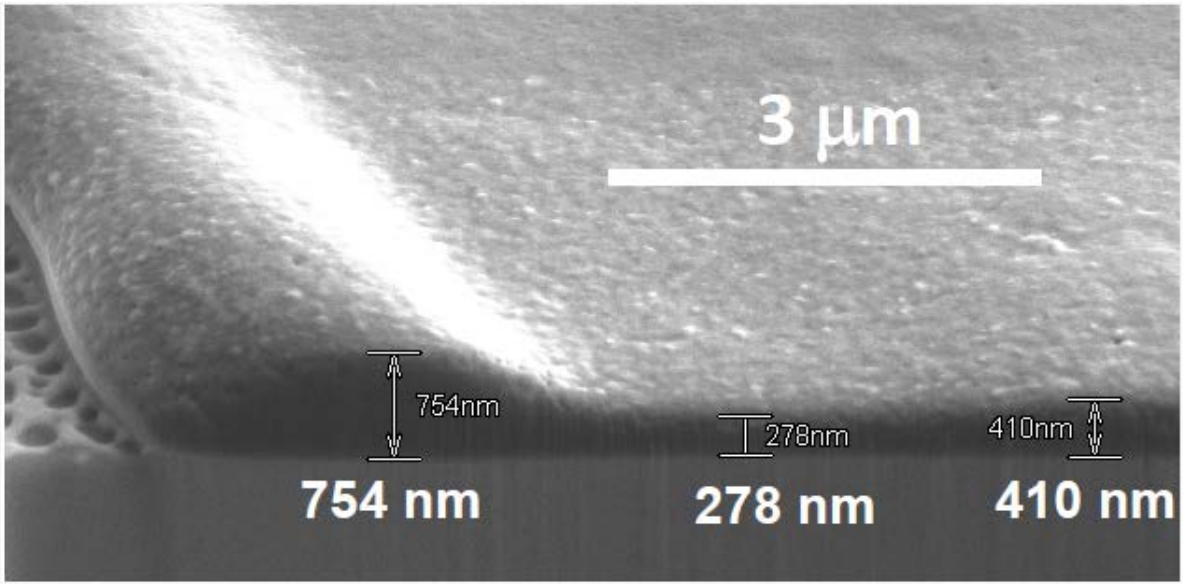

Figure 5

Figure 6

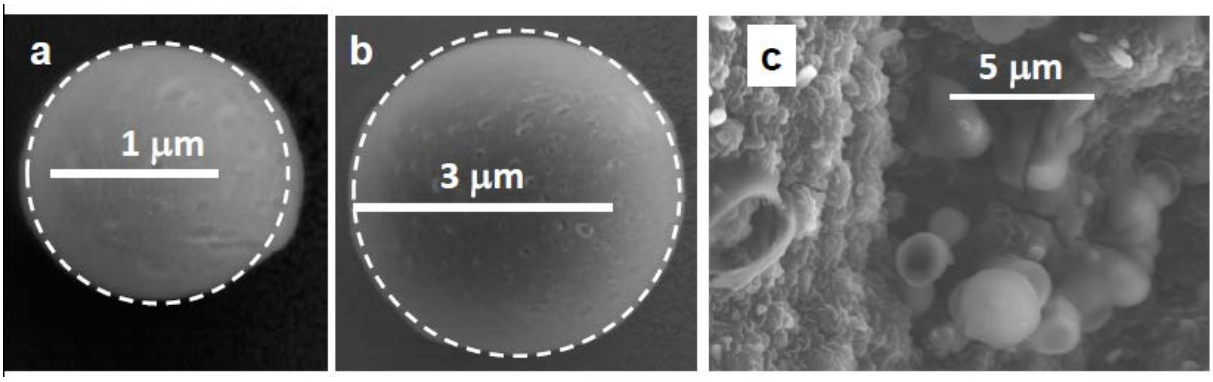

Figure 7

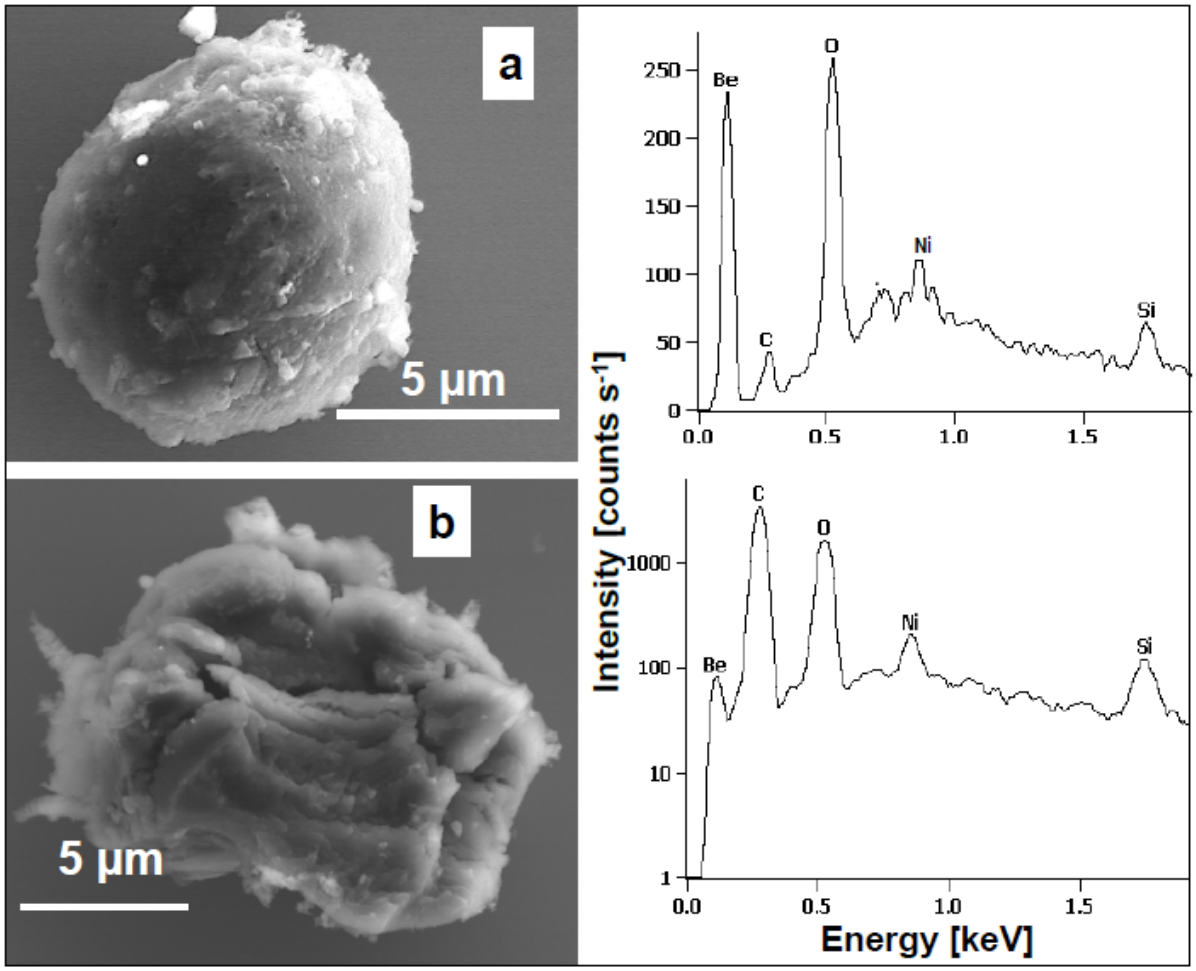

Figure 8

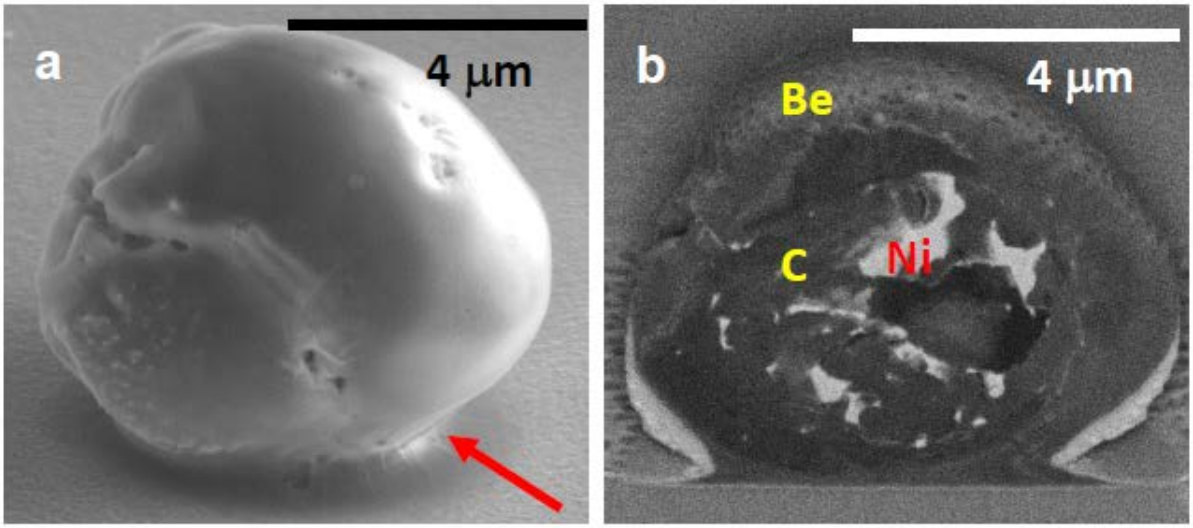

Figure 9

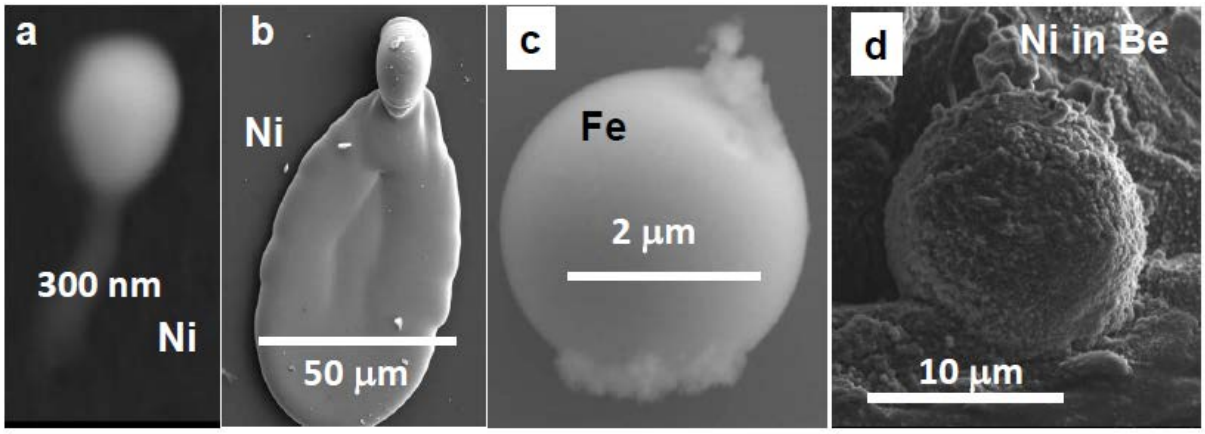

Figure 10